European Journal of Material Sciences
Vol.3, No.2, pp.64-77, May 2016
Published by European Centre for Research Training and Development UK (www.eajournals.org)

INFLUENCE OF THE LOCATION AND CRACK ANGLE ON THE MAGNITUDE OF STRESS INTENSITY FACTORS MODE I AND II UNDER UNIAXIAL TENSION STRESSES

Najah Rustum Mohsin

Southern Technical University, Technical Institute-Nasiriya, Mechanical Technics Department, Nasiriya, The_Qar, Iraq

ABSTRACT: *This paper deals with the effect of crack oblique and its location on the stress intensity factor mode I (KI) and II (KII) for a finite plate subjected to uniaxial tension stress. The problem is solved numerically using finite element software ANSYS R15 and theoretically using mathematically equations. A good agreement is observed between the theoretical and numerical solutions in all studied cases. We show that increasing the crack angle β leads to decreasing the value of KI and the maximum value of KII occurs at β=45º. Furthermore, KII equal to zero at β = 0º and 90º while KI equal to zero at β = 90º. However, there is no sensitive effect to the crack location while there is a considerable effect of the crack oblique.*

KEYWORDS: Crack, angle, location, tension, KI, KII, ANSYS R15.

INTRODUCTION

Fracture can be defined as the process of fragmentation of a solid into two or more parts under the stresses action. Fracture analysis deals with the computation of parameters that help to design a structure within the limits of catastrophic failure. It assumes the presence of a crack in the structure. The study of crack behavior in a plate is a considerable importance in the design to avoid the failure the Stress intensity factor involved in fracture mechanics to describe the elastic stress field surrounding a crack tip.

Hasebe and Inohara [1] analyzed the relations between the stress intensity factors and the angle of the oblique edge crack for a semi-infinite plate. Theocaris and Papadopoulos [2] used the experimental method of reflected caustics to study the influence of the geometry of an edge-cracked plate on stress intensity factors K_I and K_{II}. Kim and Lee [3] studied KI and KII for an oblique crack under normal and shear traction and remote extension loads using ABAQUS software and analytical approach a semi-infinite plane with an oblique edge crack and an internal crack acted on by a pair of concentrated forces at arbitrary position is studied by Qian and Hasebe [4]. Kimura and Sato [5] calculated KI and KII of the oblique crack initiated under fretting fatigue conditions. Fett and Rizzi [6] described the stress intensity factors under various crack surface tractions using an oblique crack in a semi-infinite body. Choi [7] studied the effect of crack orientation angle for various material and geometric combinations of the coating/substrate system with the graded interfacial zone. Gokul et al [8] calculated the stress intensity factor of multiple straight and oblique cracks in a rivet hole. Khelil et al [9] evaluated KI numerically using line strain method and theoretically. Recentllty, Mohsin [10 and11] studied theoretically and numerically the stress intensity factors mode I for center ,single edge and double edge cracked finite plate subjected to tension stress .

Patr´ıci and Mattheij [12] mentioned that, we can distinguish several manners in which a force may be applied to the plate which might enable the crack to propagate. Irwin proposed a

classification corresponding to the three situations represented in Figure 1. Accordingly, we consider three distinct modes: mode I, mode II and mode III. In the mode I, or opening mode, the body is loaded by tensile forces, such that the crack surfaces are pulled apart in the y direction. The mode II , or sliding mode, the body is loaded by shear forces parallel to the crack surfaces, which slide over each other in the x direction. Finally, in the mode III , or tearing mode, the body is loaded by shear forces parallel to the crack front the crack surfaces, and the crack surfaces slide over each other in the z direction,

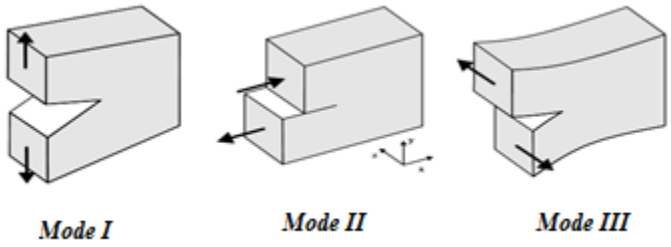

Figure 1: Three standard loading modes of a crack [12].

The stress fields ahead of a crack tip (Figure 2) for mode I and mode II in a linear elastic, isotropic material are as in the follow, Anderson [13]

Mode I:

$$\sigma_{xx} = \frac{K_I}{\sqrt{2\pi r}} \cos\left(\frac{\theta}{2}\right)\left[1 - \sin\left(\frac{\theta}{2}\right)\sin\left(\frac{3\theta}{2}\right)\right] \quad \text{……..(1)}$$

$$\sigma_{yy} = \frac{K_I}{\sqrt{2\pi r}} \cos\left(\frac{\theta}{2}\right)\left[1 + \sin\left(\frac{\theta}{2}\right)\sin\left(\frac{3\theta}{2}\right)\right] \quad \text{……..(2)}$$

$$\sigma_{xy} = \frac{K_I}{\sqrt{2\pi r}} \cos\left(\frac{\theta}{2}\right)\sin\left(\frac{\theta}{2}\right)\cos\left(\frac{3\theta}{2}\right) \quad \text{……..…..(3)}$$

Mode II:

$$\sigma_{xx} = \frac{-K_{II}}{\sqrt{2\pi r}} \sin\left(\frac{\theta}{2}\right)\left[2 + \cos\left(\frac{\theta}{2}\right)\cos\left(\frac{3\theta}{2}\right)\right] \quad \text{……..(4)}$$

$$\sigma_{yy} = \frac{K_{II}}{\sqrt{2\pi r}} \sin\left(\frac{\theta}{2}\right)\cos\left(\frac{\theta}{2}\right)\cos\left(\frac{3\theta}{2}\right) \quad \text{……..(5)}$$

$$\sigma_{xy} = \frac{K_{II}}{\sqrt{2\pi r}} \cos\left(\frac{\theta}{2}\right)\left[1 - \sin\left(\frac{\theta}{2}\right)\sin\left(\frac{3\theta}{2}\right)\right] \quad \text{……..(6)}$$

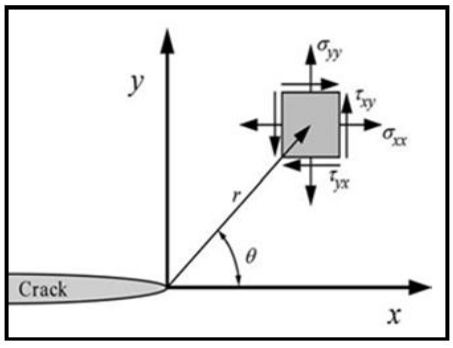

Figure 2: Definition of the coordinate axis ahead of a crack tip [13]

In many situations, a crack is subject to a combination of the three different modes of loading, I, II and III. A simple example is a crack located at an angle other than 90º to a tensile load: the tensile load σ_o, is resolved into two component perpendicular to the crack, mode I, and parallel to the crack, mode II as shown in Figure 3. The stress intensity at the tip can then be assessed for each mode using the appropriate equations, Rae [14].

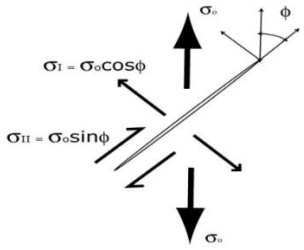

Figure 3: Crack subjected to a combination of two modes of loading I and II [14].

Stress intensity solutions are given in a variety of forms, K can always be related to the through crack through the appropriate correction factor, Anderson [13]

$$K(I, II, III) = Y\sigma\sqrt{\pi a}\,, \quad \ldots\ldots\ldots\ldots\ldots\ldots(7)$$

where σ: characteristic stress, a: characteristic crack dimension and Y: dimensionless constant that depends on the geometry and the mode of loading.

We can generalize the angled through-thickness crack of Figure 4 to any planar crack oriented $90° - \beta$ from the applied normal stress. For uniaxial loading, the stress intensity factors for mode I and mode II are given by

$$KI = KI_0 \,.\cos^2\beta \quad \ldots\ldots\ldots\ldots\ldots\ldots(8)$$

$$KII = KI_0 .\cos\beta.\sin\beta\,, \quad \ldots\ldots\ldots\ldots\ldots(9)$$

where KI_0 is the mode I stress intensity when $\beta = 0$. The crack-tip stress fields (in polar coordinates) for the mode I portion of the loading are given by

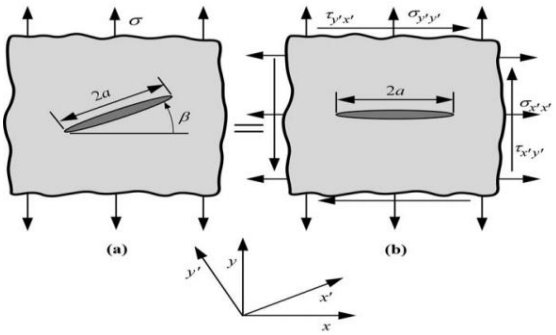

Figure 4: Through crack in an infinite plate for the general case where the principal stress is not perpendicular to the crack plane[13].

MATERIALS AND METHODS

Based on the assumptions of Linear Elastic Fracture Mechanics LEFM and plane strain problem, KI and KII to a finite cracked plate for different angles and locations under uniaxial tension stresses are studied numerically and theoretically.

Specimens Material

The plate specimen material is Steel (structural) with modulus of elasticity 2.07E5 Mpa and poison's ratio 0.29, Young and Budynas [15]. The models of plate specimens with dimensions are shown in Figure 5.

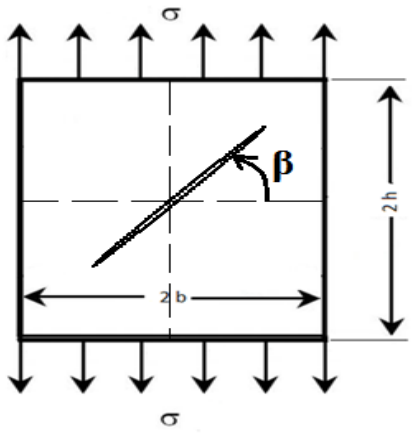

Figure 5: Cracked plate specimens.

Theoretical Solution

Values of KI and KII are theoretically calculated based on the following procedure

a) Determination of the KI_o (KI when $\beta = 0$) based on (7), where (Tada et al [16])

$$Y = \left[\sqrt{\sec\left(\frac{\pi a}{2b}\right)}\left[1 - 0.025\left(\frac{a}{b}\right)^2 + 0.06\left(\frac{a}{b}\right)^4\right]\right] \quad \text{.....(10)}$$

b) Calculating KI and KII to any planer crack oriented (β) from the applied normal stress using (8) and (9).

Numerical Solution

KI and KII are calculated numerically using finite element software ANSYS R15 with PLANE183 element as a discretization element. ANSYS models at $\beta=0^o$ are shown in Figure 6 with the mesh, elements and boundary conditions.

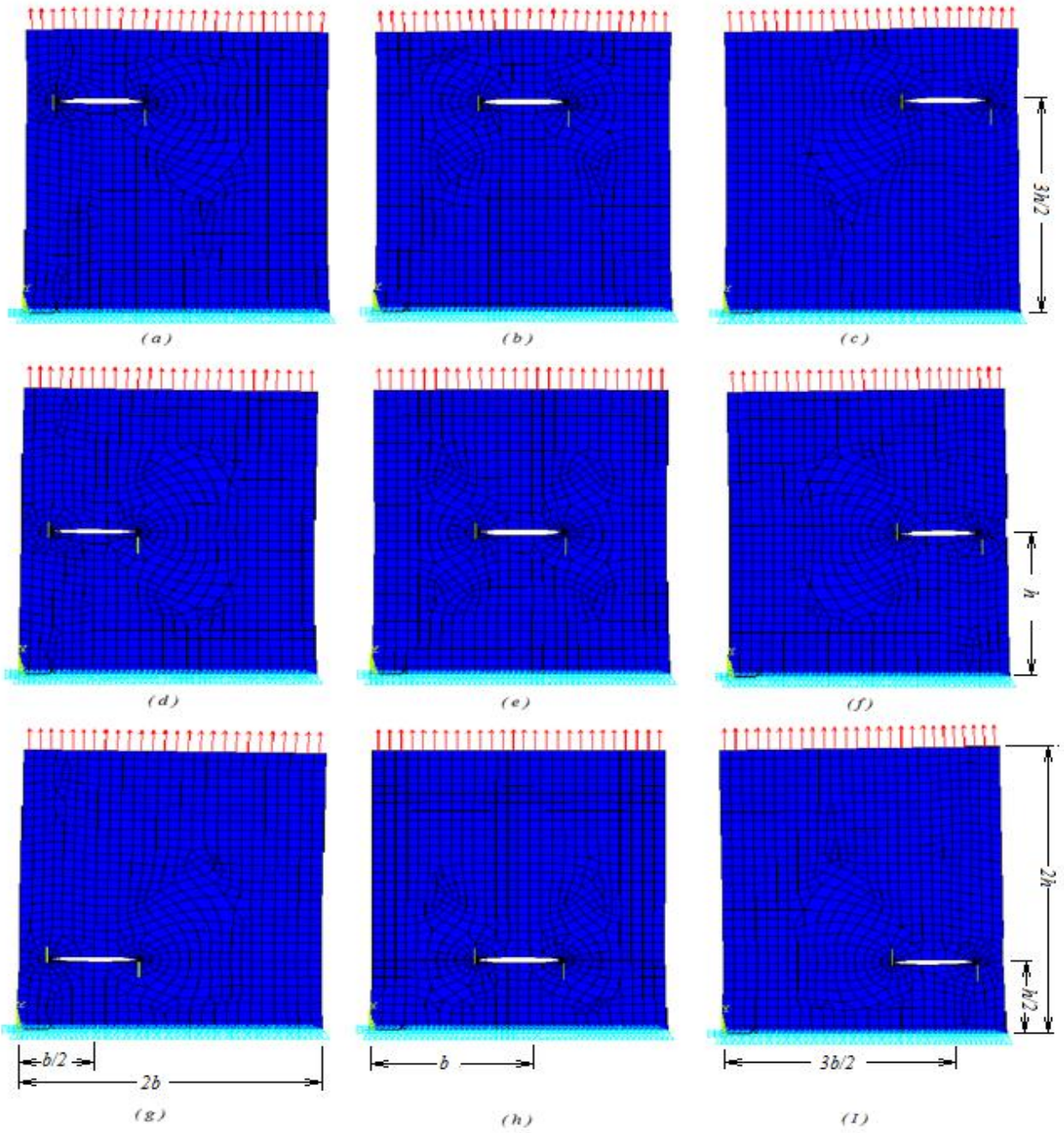

Figure 6: ANSYS models with mesh, elements and boundary conditions.

PLANE183 Description

PLANE183 is used in this paper as a discretization element with quadrilateral shape, plane strain behavior and pure displacement formulation. PLANE183 element type is defined by 8 nodes (I, J, K, L, M, N, O, P) or 6 nodes (I, J, K, L, M, N) for quadrilateral and triangle element, respectively having two degrees of freedom (Ux , Uy) at each node (translations in the nodal X and Y directions) [17]. The geometry, node locations, and the coordinate system for this element are shown in Figure 7.

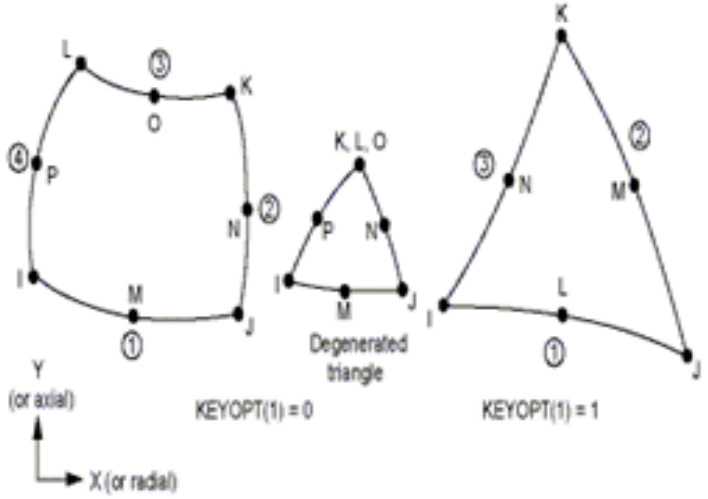

Figure 7: The geometry, node locations, and the coordinate system for element PLANE183 [17].

The Studied Cases

To explain the effect of crack oblique and its location on the KI and KII, many cases (reported in Table 1) are studied theoretically and numerically.

Table 1: The cases studied with the solution types, models and parameters.

No. of Studied Cases	Type of Solution	Changed Parameter in this Case Study		Location of the crack	No. of Figures		Other Parameters
		Name	Values				
I	Theoretical and Numerical	a/b	0.25, 0.3, 0.35, 0.4, 0.45, 0.5, 0.55, 0.6, 0.7	Model e	Figure 8a	β=0°	σ_t =200 Mpa 2b = 0.1 m 2h = 0.125 m
					Figure 8b	β=15°	
					Figure 8c	β=30°	
					Figure 8d	β=40°	
					Figure 8e	β=45°	
					Figure 8f	β=50°	
					Figure 8g	β=60°	
					Figure 8h	β=70°	
					Figure 8i	β=75°	
II	Theoretical and Numerical	a/b	0.25, 0.3, 0.35, 0.55, 0.6, 0.7	Model b	Figure 9a	β=30°	σt =200 Mpa 2b = 0.1 m 2h = 0.125 m
				Model e	Figure 9b		
				Model h	Figure 9c		
				M0del b	Figure 9d	β=45°	σt =200 Mpa 2b = 0.1 m 2h = 0.125 m
				Model e	Figure 9e		
				Model h	Figure 9f		
				Model b	Figure 9g	β=60°	σt =200 Mpa 2b = 0.1 m 2h = 0.125 m
				Model e	Figure 9h		
				Model h	Figure 9i		
III	Theoretical and Numerical	β	0°, 15°, 30°, 45°, 60°, 75°	Model b, e, h	Figure10a	KI	σt =200 Mpa 2b = 0.1 m 2h = 0.125 m a/b = 0.3
				Model b, e, h	Figure 10b	KII	
				Model d, e, f	Figure 10c	KI	
				Model d, e, f	Figure 10d	KII	

RESULTS AND DISCUSSIONS

KI and KII values are theoretically calculated by (7 - 10) and numerically using ANSYS R15 with three cases as shown in Table 1.

Case Study I

Figures 8a, b, c, d, e, f, g, h and i explain the numerical and theoretical variations of KI and KII with different values of a/b ratio when $\beta = 0^o$, 15^o, 30^o, 40^o, 45^o, 50^o, 60^o, 70^o and 75^o, respectively. From these figures, it is too easy to see that the KI > KII when $\beta < 45^o$ while KI < KII when $\beta > 45^o$ and KI ≈ KII at $\beta = 45^o$.

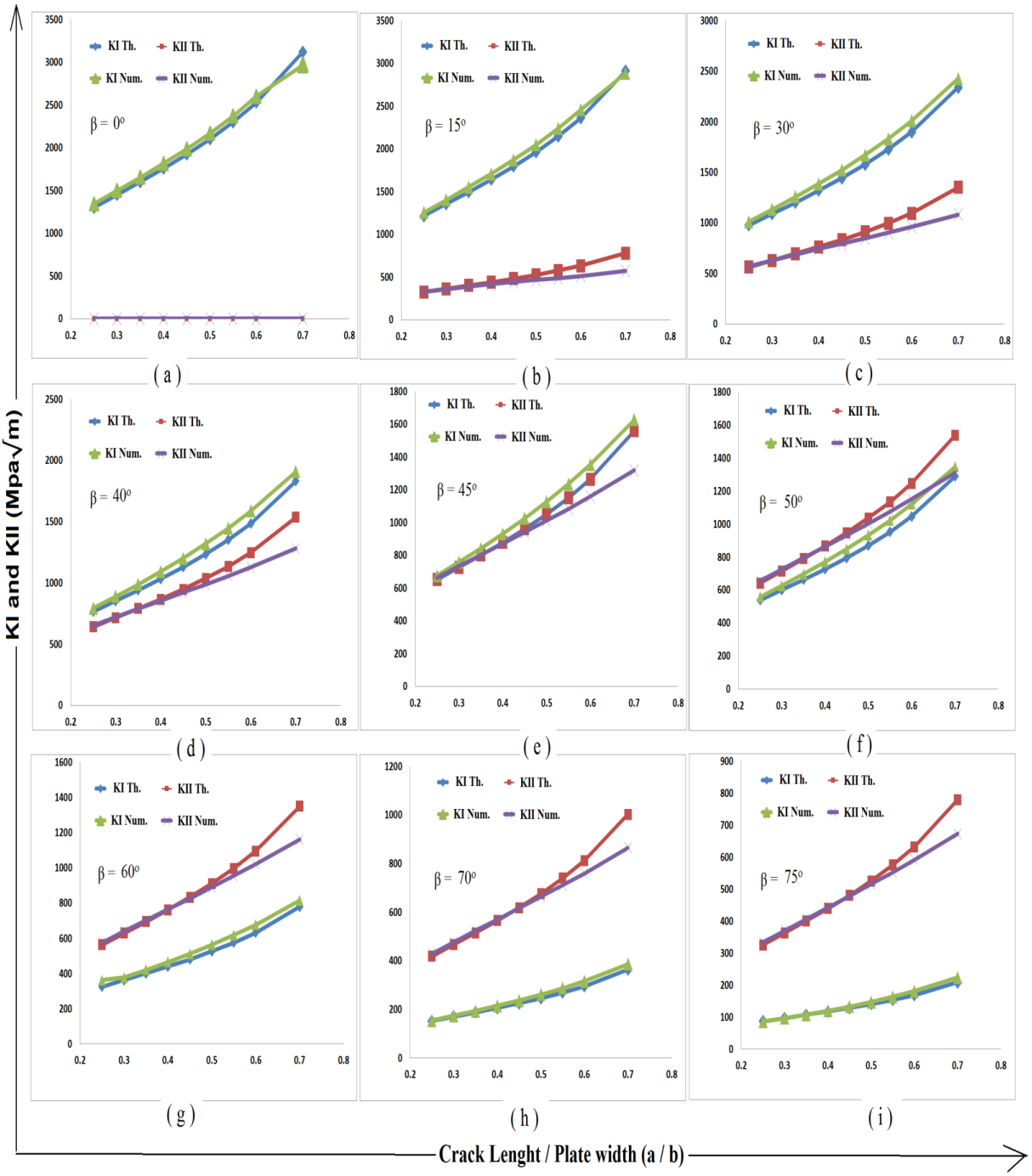

Figure 8: Variation of KI Num., KI Th., KII Num. and KII Th. with the variation of a / b and β for model e .

Case Study II

A compression between KI and KII values for different crack locations (models b, e and h) at β=30°, 45° and 60° with variations of a/b ratio are shown in Figures 9a, b, c, d, e, f, g, h and i. From these figures, it is clear that the crack angle has a considerable effect on the KI and KII values but the effect of crack location is insignificant.

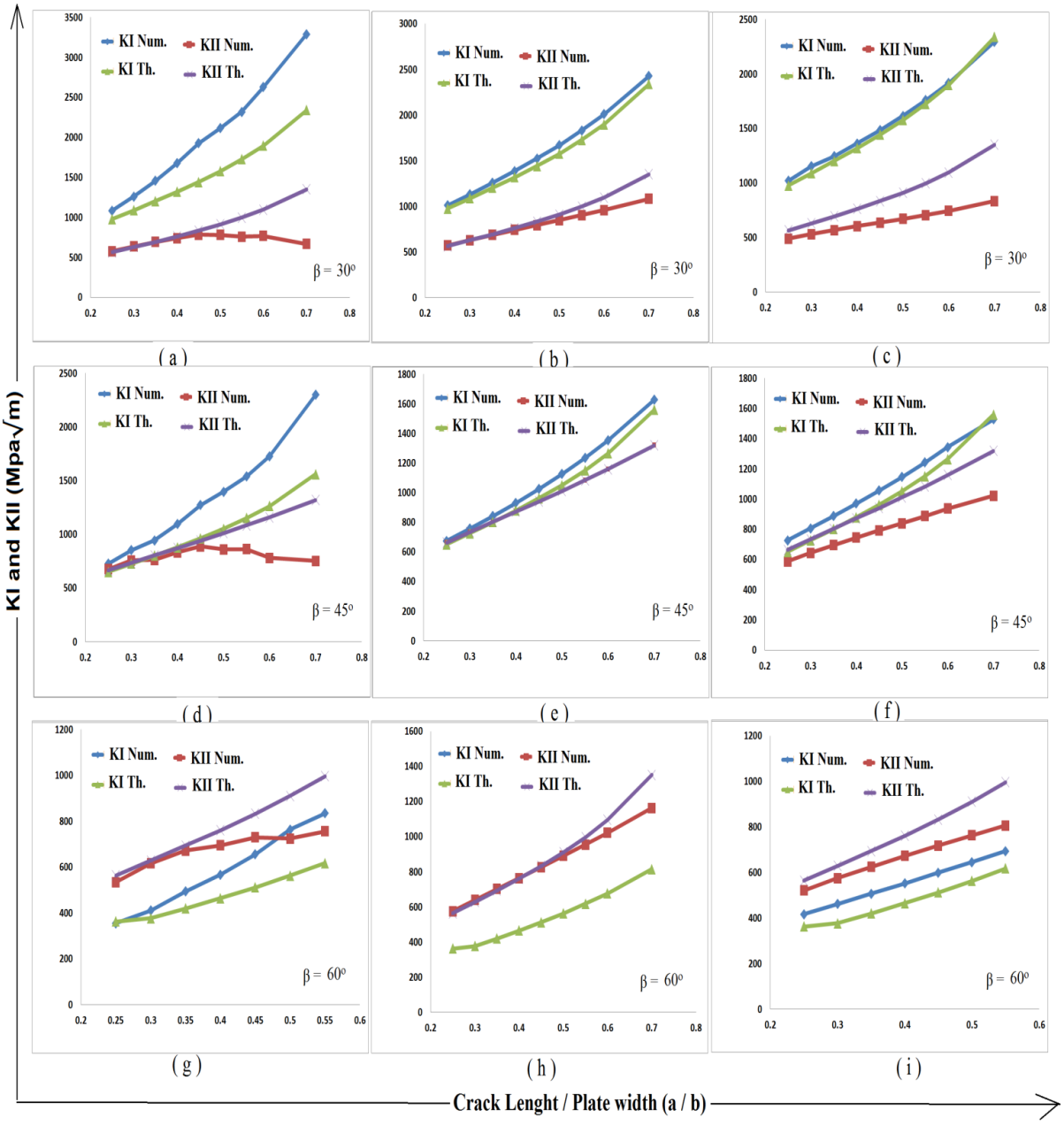

Figure 9: Variation of KI Num., KI Th., KII Num. and KII Th. with the variation of a / b for b, e and h model at β = 30, 45 and 60.

Case Study III

Figures 10a, b, c and d explain the variations of KI and KII with the crack angle β = 0°, 15°, 30°, 45°, 60°, 75° and 90° for models b, e and h. From these figures, we show that the maximum KI and KII values appear at β=0° and β=45°, respectively. Furthermore, KII equal to zero at β = 0° and β = 90°. Generally, the maximum values of the normal and shear stresses occur on surfaces where the β=0° and β=45°, respectively.

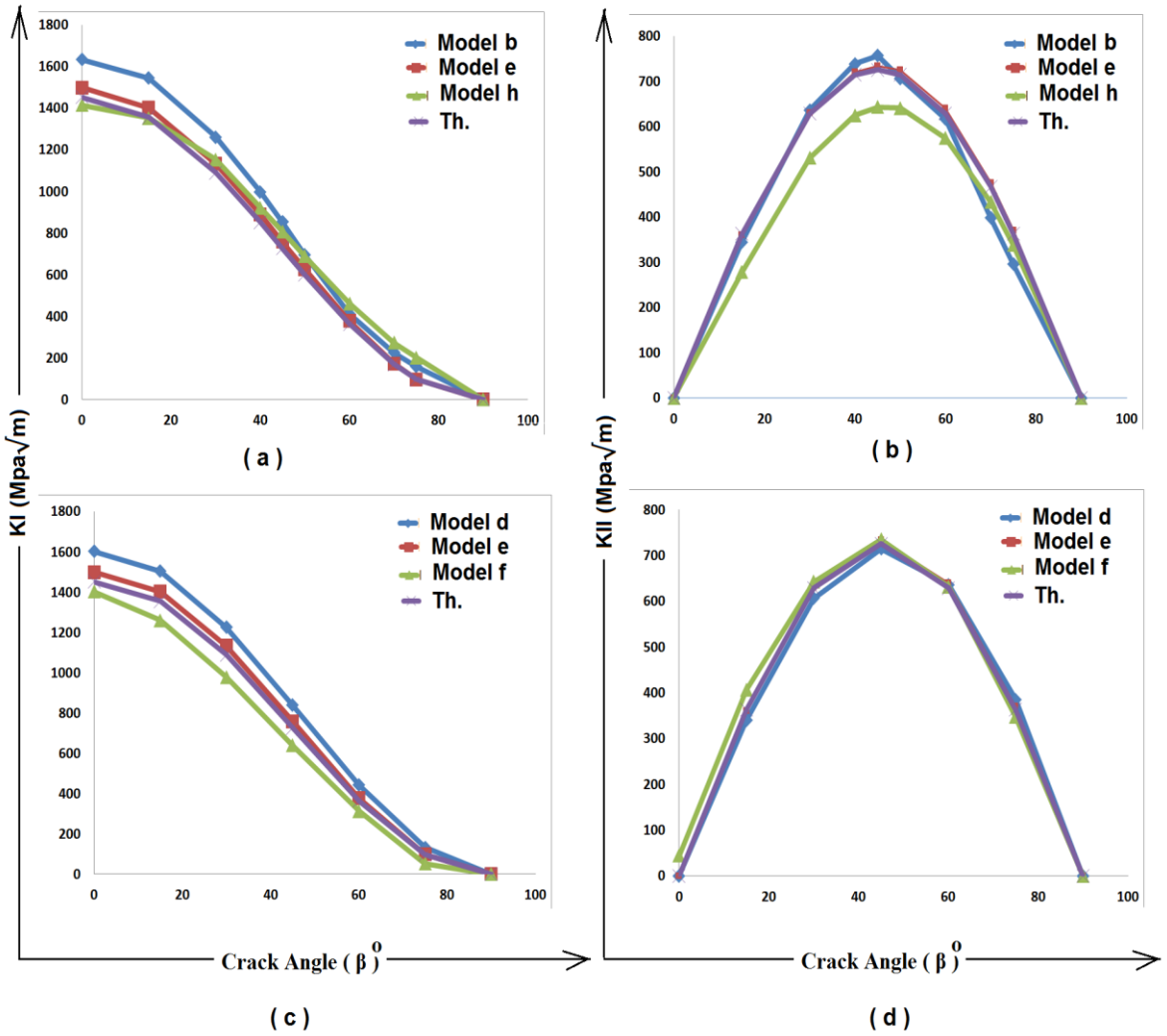

Figure 10: Variation of KI and KII with the crack angle: a and b) for model b, e, h and theoretical. c and d) for model d, e, f and theoretical.

From all figures, it can be seen that there is no significant difference between the theoretical and numerical solutions.

Furthermore, Figures 11 and 12 are graphically illustrated Von-Mises stresses countor plots with the variation of location and angle of the crack, respectively. From these figures, it is clear that the effect of crack angle and the effect of crack location are incomparable.

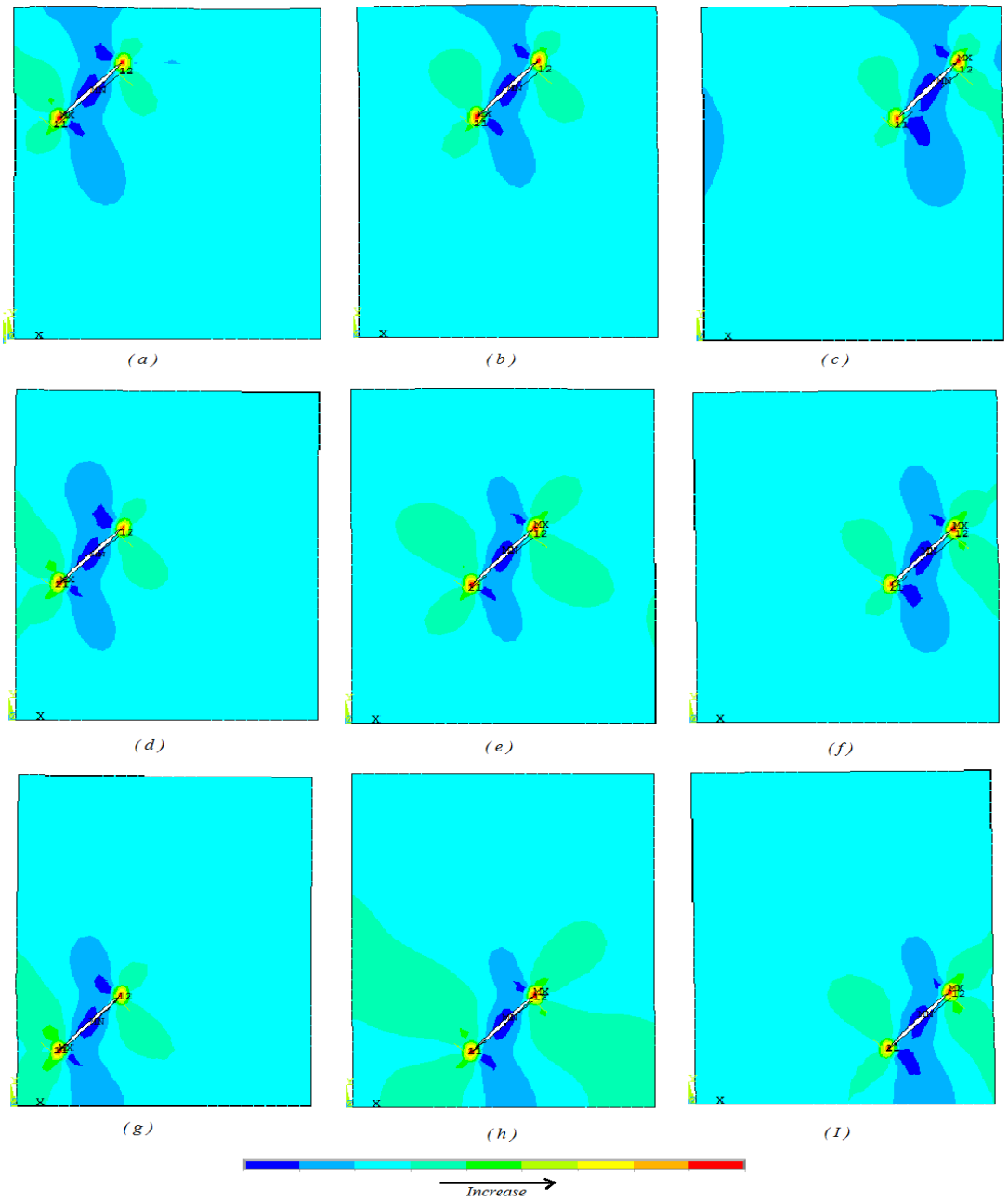

Figure 11: Countor plots of Von-Mises stress with the variation of crack location at β = 45º.

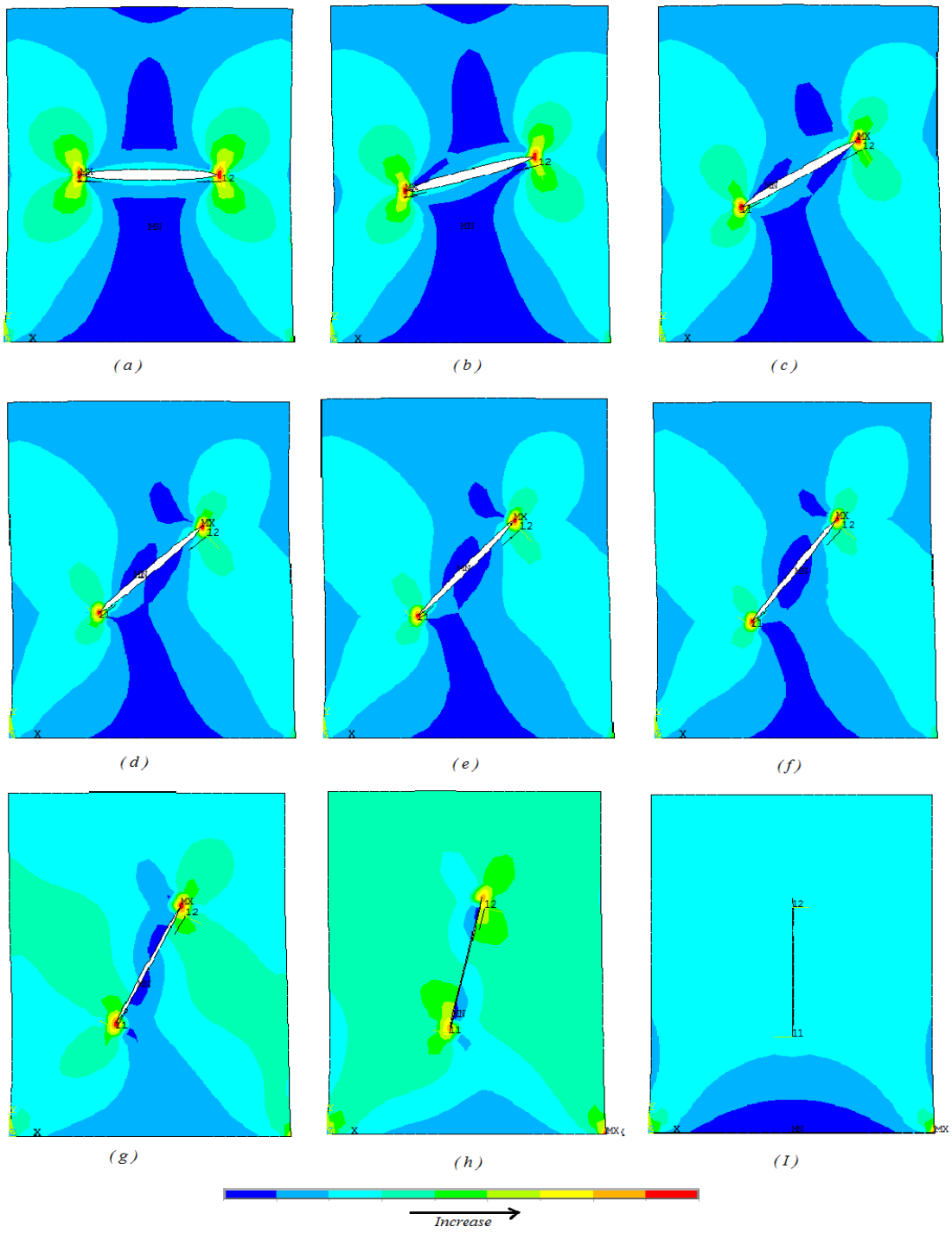

Figure 12: Countor plots of Von-Mises stress with the variation of crack angle at specific location.

CONCLUSIONS

1) A good agreement is observed between the theoretical and numerical solutions in all studied cases.

2) Increasing the crack angle β leads to decrease the value of K_I and the maximum value of KII occurs at β=45.

3) KII vanished at β = 0° and 90° while KI vanished at β = 90°.

4) There is no obvious effect to the crack location but there is a considerable effect of the crack oblique.

REFERENCES

N. Hasebe and S. Inohara. Stress Analysis of a Semi-Infinite Plate with an Oblique Edge Crack. Ingenieur-Archiv, Volume 49(1), pp. 51-62, 1980.

P. S. Theocaris and G. A. Papadopoulos. The Influence of Geometry of Edge-Cracked Plates on KI and KII Components of the Stress Intensity Factor. Journal of Physics D: Applied Physics. Vol. 17(12), pp. 2339-2349, 1984.

H.K. Kim and S.B. Lee. Stress intensity factors of an oblique edge crack subjected to normal and shear tractions. Theoretical and Applied Fracture Mechanics, Volume 25(2), pp. 147–154, 1996.

J. Qian and N. Hasebe. An Oblique Edge Crack and an Internal Crack in a Semi-Infinite Plane Acted on by Concentrated Force at Arbitrary Position. Engineering Analysis with Boundary Elements, Vol. 18, pp. 155-16, 1996.

T. Kimura and K. Sato. Simplified Method to Determine Contact Stress Distribution and Stress Intensity Factors in Fretting Fatigue. International Journal of Fatigue, Vol. 25, pp. 633–640, 2003.

T. Fett and G. Rizzi. Weight Functions for Stress Intensity Factors and T-Stress for Oblique Cracks in a Half-Space. International Journal of Fracture, Vol. 132(1), pp. L9-L16, 2005.

H. J. Choi. Stress Intensity Factors for an Oblique Edge Crack in a Coating/Substrate System with a Graded Interfacial Zone under Antiplane Shear. European Journal of Mechanics A/Solids. Vol. 26, pp. 337–3, 2007.

Gokul.R , Dhayananth.S , Adithya.V, S.Suresh Kumar. Stress Intensity Factor Determination of Multiple Straight and Oblique Cracks in Double Cover Butt Riveted Joint. International Journal of Innovative Research in Science, Engineering and Technology, Vol. 3(3), 2014.

F. Khelil, M. Belhouari, N. Benseddiq, A. Talha. A Numerical Approach for the Determination of Mode I Stress Intensity Factors in PMMA Materials. Engineering, Technology and Applied Science Research, Vol. 4(3), 2014.

N. R. Mohsin. Static and Dynamic Analysis of Center Cracked Finite Plate Subjected to Uniform Tensile Stress using Finite Element Method. International Journal of Mechanical Engineering and Technology (IJMET), Vol. 6, (1), pp. 56-70, 2015.

N. R. MOHSIN. Comparison between Theoretical and Numerical Solutions for Center, Single Edge and Double Edge Cracked Finite Plate Subjected to Tension Stress. International Journal of Mechanical and Production Engineering Research and Development (IJMPERD), Vol. 5(2), pp. 11-20, 2015.

M. Patr´ıci and R. M. M. Mattheij. Crack Propagation Analysis, http://www.win.tue.nl/analysis/reports/rana07-23.pdf .

T.L.Anderson. Fracture Mechanics Fundamentals and Applications. Third Edition, Taylor &Francis Group, CRC Press, 2005.

C. Rae. Natural Sciences Tripos Part II- MATERIALS SCIENCE- C15: Fracture and Fatigue. https://www.msm.cam.ac.uk/teaching/partII/courseC15/C15H.pdf .

W. C. Young and R. G. Budynas. Roark's Formulas for Stress and Strain. McGraw-Hill companies, Seventh Edition, 2002.

H. Tada, P. C. Paris and G. R. Irwin. The Stress Analysis of Cracks Handbook. Third edition, ASME presses, 2000.